

J. R. Beene, M. L. Halbert and D. C. Hensley
Oak Ridge National Laboratory

D. G. Sarantites, L. W. Westerberg, K. Geoffroy and R. Woodward
Washington University

The continuum gamma-ray spectrum produced by a residual deformed nucleus following a HI-induced evaporation reaction is the most promising source of experimental information on the nuclear structure of yrast and near-yrast states at very high spin (>40).¹ For a typical deformed rare-earth residue, the high-spin nuclear structure information is contained in a well localized bump of γ -radiation between a few hundred keV and ~ 1.5 MeV. The radiation in this region (at least for $E_{\gamma} > 500$ keV) is dominated by stretched E2 transitions,² and is known as the "yrast" continuum, though at high spin collective cascades up to several MeV above the yrast line probably contribute to it. Underlying this is a continuum of statistical transitions (i.e. noncollective transitions which carry away excitation energy but little spin) which are observed to have a spectral shape that is very close to exponential above $E_{\gamma} \sim 2$ MeV.

We have attempted a detailed quantitative analysis of the yrast continuum by subtracting the underlying statistical continuum in a way that makes allowance for our ignorance of its detailed shape. This procedure makes it possible to obtain the moment of inertia as a function of spin over a wide range of spins. The results of this continuum spectral shape analysis can be used to calculate the first and second moments of the continuum multiplicity distribution. Such calculations are found to be in reasonable agreement with experimental data on these quantities.

Continuum spectra were taken in 5 cm x 7.6 cm NaI detectors, in coincidence with a seven-detector NaI array, during the bombardment of ^{150}Nd by 115- and 130-MeV beams of ^{20}Ne . The spectra were unfolded to correct for detector response.

In the first stage of analysis the high energy part ($E_\gamma \geq 2.5$ MeV) of a spectrum was fit to the empirical form

$$N_S(E_\gamma) = A E_\gamma^x \exp(-E_\gamma/T) \quad \text{Eq. 1}$$

where A is a normalization constant and x and T are considered purely empirical parameters.³ The fits were made with a range of fixed values of x . Using best fit values for A and T , the resulting statistical component was subtracted from the experimental spectrum and the difference interpreted as the yrast continuum. Curves for $x = 0.5$ to 5 and some resulting yrast continua are shown in Fig. 1. For each value of x these fits give such quantities as the relative yield of yrast and statistical transitions, the average statistical γ -ray energy and the absolute statistical γ yield. Values of x outside the range ~ 1.5 to ~ 3.5 were found to give results for these quantities at variance with other experimental data. In all subsequent analyses of the yrast continua, uncertainties on deduced parameters have been expanded to span the full range of their variation with x in the range 1.5 to 3.5 .

In order to proceed with the yrast analysis, a simple picture of the yrast cascade, similar to that employed in previous work,⁴ was used. The relationship between spin (I), E_γ and moment of inertia, \mathcal{J} , was taken as

$$E_\gamma = \frac{\hbar^2}{2\mathcal{J}} (4I-2) \quad \text{Eq. 2}$$

and the spin distribution at entry:

$$P(I) \propto (2I + 1) / \left\{ 1 + \exp\left(\frac{I - I_{\max}}{d}\right) \right\} \quad \text{Eq. 3}$$

where d was taken from optical model calculations (3.5 - 4) and I_{\max} was fixed by requiring agreement with gamma multiplicity experiments.⁵ By considering only those events in which a given minimum number of detectors in the seven-NaI array fired, the upper spin region in the residue can be enhanced and low multiplicity background arising from Coulomb excitation and other quasi-elastic reactions can be removed. The effect of this requirement can be taken into account in a well-defined way as a modification of the entry spin distribution.

Using the assumed entry spin distribution, the yield of yrast gamma radiation as a function of the initial spin in the transition, $Y(I)\Delta I$, can be calculated. From this quantity and the experimental yrast-continuum yield data, $Y(E_\gamma)\Delta E_\gamma$, we can obtain an approximation for dI/dE_γ as a function of E_γ

$$\frac{dI}{dE_\gamma} \propto \frac{Y(I=f(E_\gamma, \mathcal{G})) \Delta I}{Y(E_\gamma) \Delta E_\gamma} \quad \text{Eq. 4}$$

From Eq. 2, with $k = \hbar^2/2\mathcal{I}$, we have

$$\frac{dk}{dE_\gamma} = \left[\frac{1}{4k} - \frac{dI}{dE_\gamma} \right] \frac{4k}{E_\gamma^2} \quad \text{Eq. 5}$$

These equations can be integrated numerically to give I vs. E_γ or equivalently k vs. E_γ or I , provided a value of E_γ is available at which k and dk/dE_γ are known (for example, a point of approximately constant \mathcal{G} , where $dk/dE_\gamma = 0$). This procedure has been applied to the 130- and 115-MeV data using known values of \mathcal{G} at high spin from the ^{164}Yb ground state band.⁶ Results obtained from the sum of four-and-higher fold data are shown⁷ in Fig 2a. These results are reproduced schematically in Fig. 2b, together with values deduced from a conventional integral analysis.⁸ Also shown are contributions of various final channels to different spin regions, deduced from multiplicity distribution measurements.⁵ The 130-MeV data show the moment of inertia to rise slowly with spin over the full range for which our data can be considered meaningful, reaching the rigid sphere value at $I \sim 50$. The flattening in the 115-MeV data at lower spin is probably related to increasing yield in the 5n channel at high spin in those data.

We have also studied the first and second moments of the γ -ray multiplicity distribution as a function of E_γ with a setup similar to that described above, but with spectral information derived from a conversion electron lens.⁹ The resulting data are shown in Fig. 3 for 130 MeV $^{20}\text{Ne} + ^{150}\text{Nd}$. The parameters deduced in the spectral shape analysis outlined above were used to make the calculations shown as solid lines, with the only additional input being the assumption that the average

statistical multiplicity is constant with a value chosen to fit high E data. The $x = 2$ results were used in this calculation; smaller and larger³ values of x give in appreciably poorer accounts of the data. Somewhat better agreement with the data is obtained by assuming a larger value of the spin population diffuseness than was used in the spectral shape analysis, as shown by the dotted lines in Fig. 3. The bump in μ data near 1.5 MeV does not imply any unusual characteristics of the entrance spin distribution, but arises from the mixture near this energy of very high multiplicity yrast transitions with comparable numbers of relatively low $\langle M \rangle$ statistical transitions leading to a double humped (and hence broad) multiplicity distribution.

REFERENCES

- * Research sponsored by the Division of Basic Energy Sciences of the U. S. Department of Energy, under contract W-7405-eng-26 with Union Carbide Corporation.
1. See for example Hubel et al., Phys. Rev. Lett. 41, 791 (1978), and references to the extensive work of Stephens, Diamond, Newton and collaborators therein.
 2. M. Deleplanque et al., Phys. Rev. Lett. 41, 1105 (1978) and L. Westerberg et al., Phys. Rev. Lett. 41, 96 (1978).
 3. In a simple picture of the statistical gamma decay of a level at excitation energy E , one might expect a spectral distribution of primary radiation of multipolarity, L , of the form^{10,11} $N(E) \propto E^{2L+1} S(E, L) \exp(-E/T)$ ($E < E_c$). For electric dipole radiation $S(E, 1) \propto E^2$ is expected.^{10,11} Our use of smaller values of x in Eq. 1 than the $x = 5$ expected on this basis does not imply a radically different dipole strength function at high spin. Rather, if secondary and subsequent radiation is considered, a considerable excess of low E radiation over that predicted for the primary spectrum results. This could lead to the small effective values of x in our analysis.
 4. M. Deleplanque et al., Phys. Rev. Lett. 40, 625 (1978).
 5. D. G. Sarantites et al., Phys. Rev. C14, 2138 (1976).
 6. N. R. Johnson, Private Communication.
 7. The failure of the analysis to reproduce rapid variation in μ at low spin is to be expected because of the comparatively large bin width ($\Delta E = 0.1$ MeV) in the data. In addition, the reliability of the data below $E = 300$ -400 keV is uncertain.
 8. R. S. Simon et al., Phys. Rev. Lett. 36, 359 (1976).
 9. L. Westerberg et al., Nucl. Instrum. Meth. 145, 295 (1977).
 10. G. A. Bartholemew et al., Advances in Nuclear Physics, Vol. 7, Baranger and Vogt eds., (Plenum Press, New York, 1973) p. 229.
 11. R. M. Lieder and H. Ryde, Advances in Nuclear Physics, Vol. 10, Baranger and Vogt eds., (Plenum Press, New York, 1978) p. 1.

FIGURE CAPTIONS

- Fig. 1 Statistical continuum fits and deduced yrast continua.
- Fig. 2 Moment of inertia vs. spin for 115- and 130-MeV $^{20}\text{Ne} + ^{150}\text{Nd}$. Results⁶ of the analysis at both energies is shown in Fig. 2a. In Fig. 2b, these results are schematically reproduced along with an indication of the contribution of various final channels. The solid line in 2a is for the ground band in ^{164}Yb deduced from discrete line spectra (preliminary results, Ref. 6).
- Fig. 3 Mean and width of the multiplicity distribution for 130-MeV $^{20}\text{Ne} + ^{150}\text{Nd}$. The solid lines are for $x = 2$, $d = 3.5$ and the dashed lines for $x = 2$, $d = 8$.

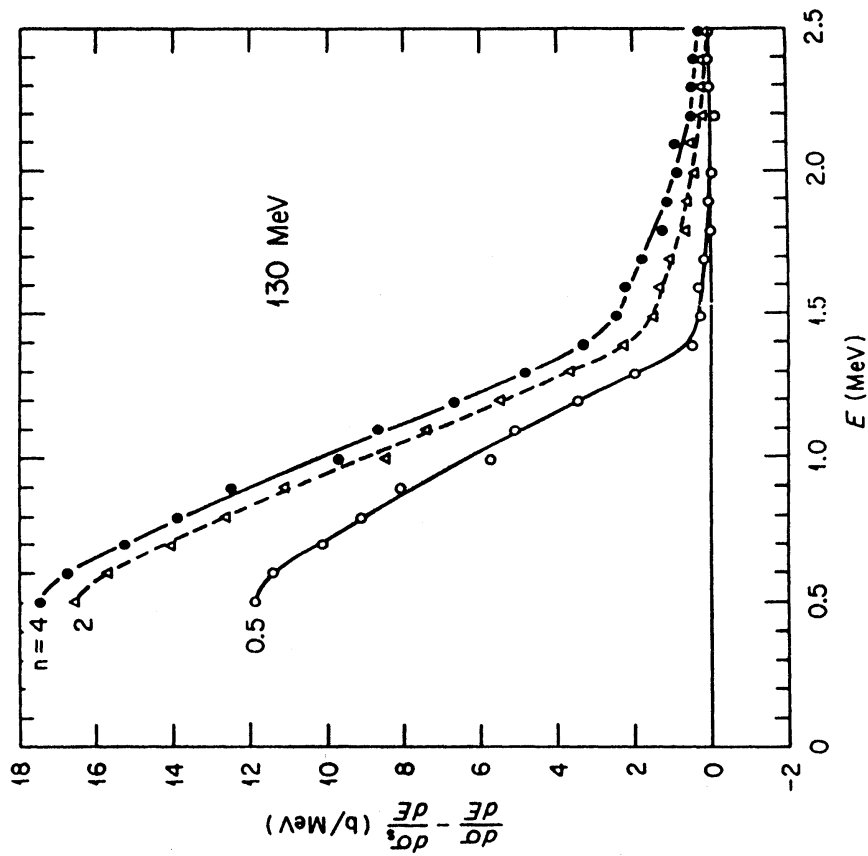
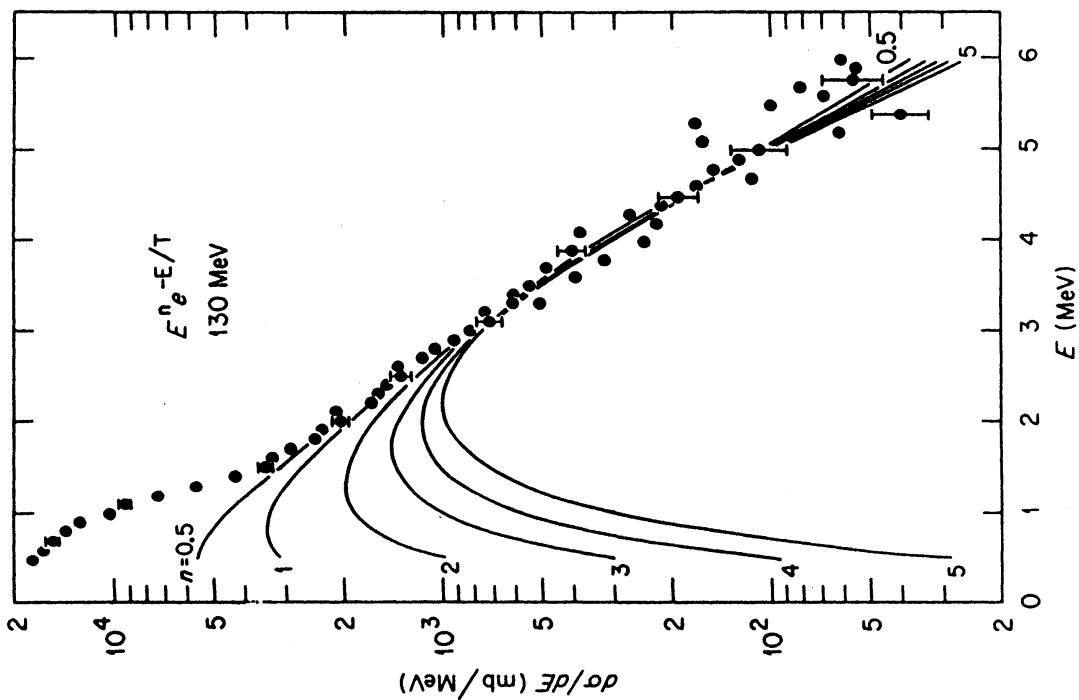


Fig. 1a

Fig. 1b

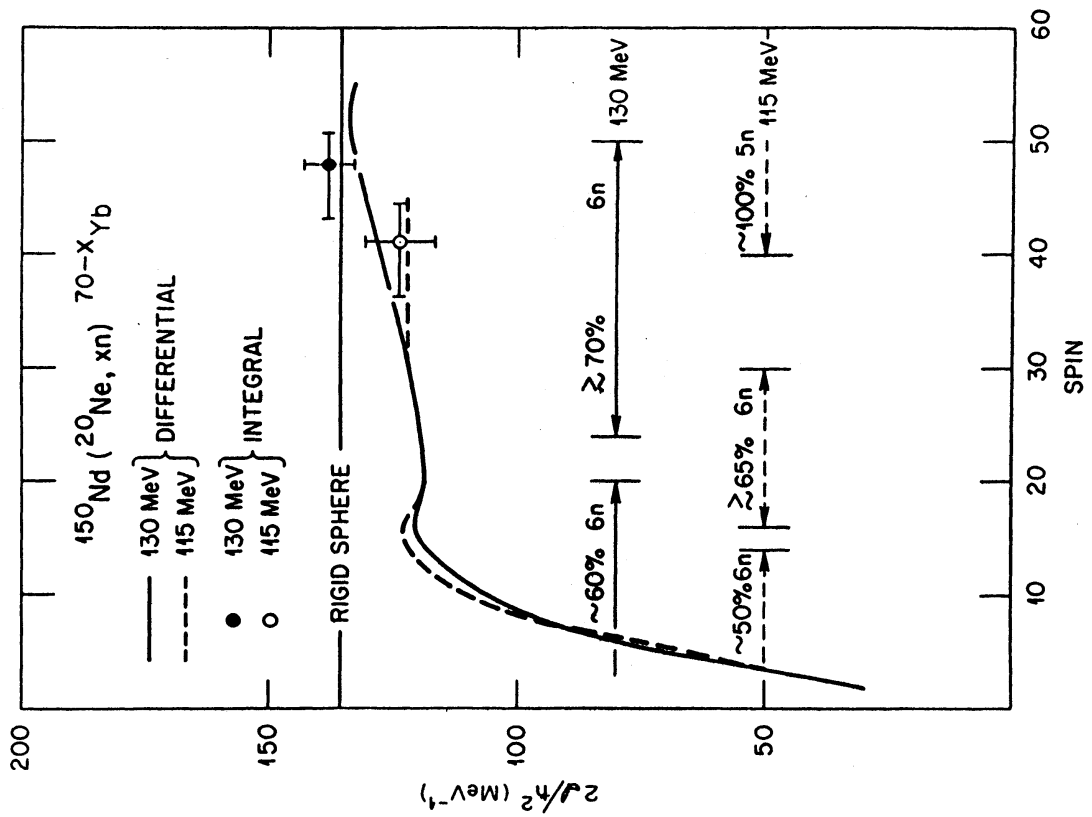


Fig. 2b

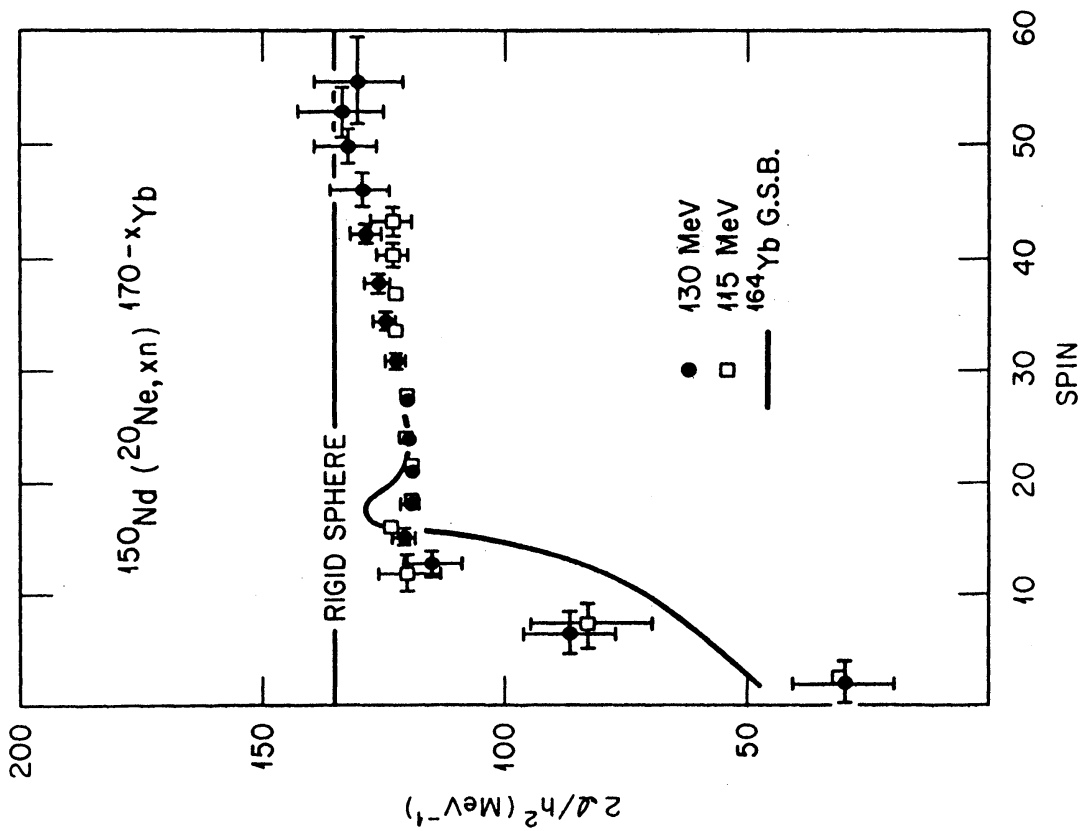


Fig. 2a

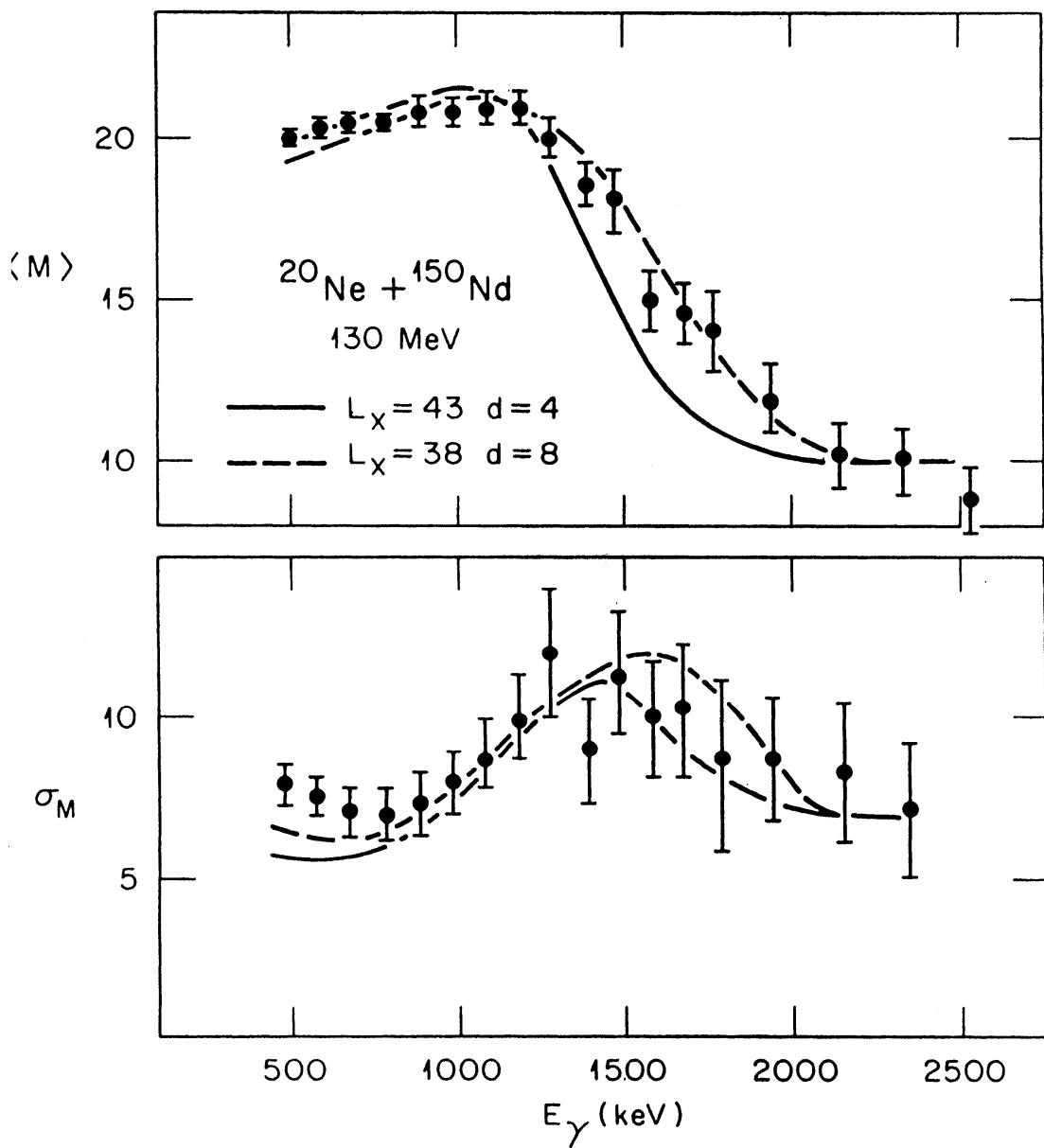


Fig. 3